

# Ion heating in the Globus-M2 tokamak using the hydrogen and deuterium neutral beams injection

© G.S. Kurskiev<sup>1</sup>, I.V. Miroshnikov<sup>1</sup>, N.V. Sakharov<sup>1</sup>, V.K. Gusev<sup>1</sup>, V.B. Minaev<sup>1</sup>, Yu.V. Petrov<sup>1</sup>, A.Yu. Telnova<sup>1</sup>, N.N. Bakharev<sup>1</sup>, E.O. Kiselev<sup>1</sup>, N.S. Zhiltsov<sup>1</sup>, P.B. Shchegolev<sup>1</sup>, I.M. Balachenkov<sup>1</sup>, V.I. Varfolomeev<sup>1</sup>, A.V. Voronin<sup>1</sup>, V.Yu. Goryainov<sup>1</sup>, A.A. Kavin<sup>2</sup>, S.V. Krikunov<sup>1</sup>, A.D. Melnik<sup>1</sup>, A.B. Mineev<sup>2</sup>, A.N. Novokhatskii<sup>1</sup>, M.I. Patrov<sup>1</sup>, A.M. Ponomarenko<sup>3</sup>, O.M. Skrekel<sup>1</sup>, V.A. Solovey<sup>4</sup>, V.V. Solokha<sup>1</sup>, E.E. Tkachenko<sup>1</sup>, V.A. Tokarev<sup>1</sup>, S.Yu. Tolstyakov<sup>1</sup>, E.A. Tukhmenova<sup>1</sup>, N.A. Khromov<sup>1</sup>, F.V. Chernyshev<sup>1</sup>, K.D. Shulyatiev<sup>1</sup>, A.Yu. Yashin<sup>1,3</sup>

<sup>1</sup> Ioffe Institute, St. Petersburg, Russia

<sup>2</sup> JSC „NIIIEFA“, St. Petersburg, Russia

<sup>3</sup> Peter the Great Saint-Petersburg Polytechnic University, St. Petersburg, Russia

<sup>4</sup> St. Petersburg Nuclear Physics Institute, National Research Center Kurchatov Institute, Gatchina, Russia

E-mail: Gleb.Kurskiev@mail.ioffe.ru

Received November 14, 2024

Revised November 14, 2024

Accepted November 18, 2024

The paper is devoted to plasma heating study at the spherical tokamak Globus-M2. Injection of a deuterium beam into deuterium plasma allows obtaining significantly higher ion temperatures than in the case of hydrogen injection into deuterium plasma. In both cases the ion temperature significantly exceeds the electron temperature, and the plasma is in the so-called „hot ion mode“. The plasma energy confinement time in the case of deuterium injection is significantly higher than in the case of hydrogen injection due to the higher thermal insulation of the plasma ions.

**Keywords:** Controlled nuclear fusion, spherical tokamak, Globus-M2, neutral beam injection, hot ion mode, isotope effect.

DOI: 10.61011/TPL.2025.04.60987.20186

It was found in experiments on plasma heating at spherical tokamaks (STs) in toroidal magnetic field  $B_T < 0.55$  T that the heat transfer by ions in the H-mode is characterized well by neoclassical theory [1,2]. However, when low collisionality is reached, the development of small-scale instabilities, such as the ion temperature gradient (ITG) mode [3] or a hybrid instability combining the properties of the kinetic ballooning mode and the trapped electron mode (KBM/TEM) [4], was expected to induce a significant anomalous energy transfer by ions. The first experiments at STs with  $B_T = 0.8$  T revealed that the heat transfer by ions becomes anomalous, interfering with the growth of ion temperature to levels exceeding the electron temperature values [5,6]. However, subsequent experiments at STs with strong magnetic fields demonstrated the feasibility of heating of plasma ions in a compact tokamak to sub-thermonuclear temperatures of 4–8 keV [7–9] via neutral injection.

It has already been established that the use of two injectors for deuterium plasma heating at the Globus-M2 tokamak allows one to obtain an ion temperature exceeding the electron temperature by a factor of more than 1.5 within a wide range of average plasma electron density values of  $(1.6–10) \cdot 10^{19} \text{ m}^{-3}$  [6] (with a characteristic pronounced maximum near  $n_e \approx 5 \cdot 10^{19} \text{ m}^{-3}$ ). A more thorough analysis revealed that the maximum achievable ion temperature depends primarily on the mass of injected

high-energy atoms (Fig. 1). Let us compare two Globus-M2 discharges corresponding to different masses of injected ions and the same values of  $B_T = 0.9$  T and plasma current  $I_p = 0.35$  MA. In both cases, the injection of the first beam is initiated at the stage of plasma current growth and continues almost until the end of a discharge. The second beam remains active for 40 ms and is switched on when the plasma current reaches a plateau (Fig. 2). The power of ohmic heating in the discharges with hydrogen and deuterium injection is estimated at 0.2 and 0.17 MW, respectively. These values are significantly lower than the introduced additional heating power, which is 1.35 and 1.15 MW in the former and the latter cases, respectively. Injected power losses are largely attributable to the loss of fast ions from uncontrolled orbits and in the process of their deceleration due to charge exchange with neutral particles. The absorbed beam power calculated by the NUBEAM code is 0.54–0.81 MW for the deuterium beam and 0.85–1.15 MW for the hydrogen one (depending on the density of neutral particles). The ion temperature measured by the charge exchange recombination spectroscopy (CXRS) diagnostics with a time resolution of 5 ms increases from the moment of injection of the second beam, exceeding significantly the electron temperature measured by the Thomson scattering diagnostics. Both discharges feature sawtooth oscillations. After each reconnection,

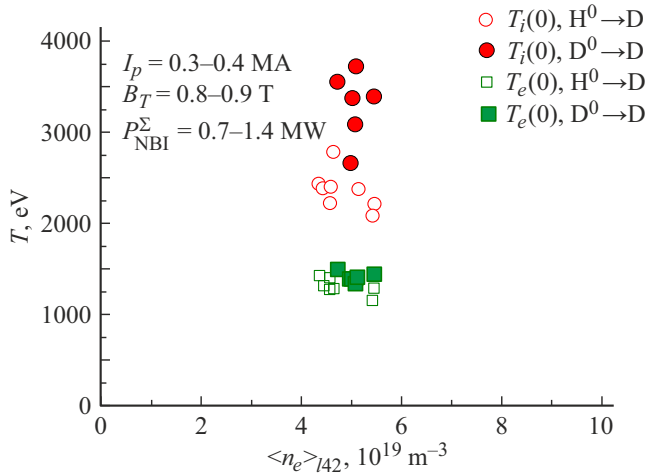


**Figure 1.** Averaged values of temperature of electrons and ions in the central region of plasma with heating of deuterium plasma by hydrogen and deuterium beams. Each point corresponds to a separate discharge; the presented values were also averaged over several time points. Hydrogen injection: discharges Nos. 42122, 42119, 42089, 42121, 42341, 42325, and 42341. Deuterium injection: discharges Nos. 42777, 42703, 42368, 42767, 41585, and 42416.

rapidly damped oscillations are observed at the magnetic probes within the  $\sim 30$  kHz frequency range, presumably with mode numbers  $m = 2$ ,  $n = 1$  ( $2/1$ ). The nature of magnetohydrodynamic oscillations in the discharge with deuterium injection differs slightly. At the end of the discharge (after 0.22 s), the duration and amplitude of oscillations increase, and instability is observed until the onset of the next period of sawtooth oscillations; alongside with that, the ion temperature decreases from 4 to 2.5 keV.

Let us choose a time point near the maximum ion temperature (Fig. 3) in order to compare the spatial temperature distributions and perform further analysis of the plasma energy balance. It can be seen that the maximum measured ion temperatures with deuterium beam injection reach 4 keV, which is significantly higher than the values corresponding to heating by the hydrogen beam. At the same time, the electron temperature and density do not differ in any significant way (Figs. 2 and 3). The values of energy stored by plasma electrons and ions determined from the kinetic diagnostics data are given in the table. It follows from the table that a significant fraction of the total thermal energy stored in plasma is attributable to ions. It varies from 48 % with hydrogen injection to 60 % in the case of deuterium injection. The plasma heating power was calculated by the NUBEAM code [10] for different values of the neutral particle density, which was a free parameter in modeling and the main source of uncertainty in the calculation results (see the table). With deuterium beam injection, the energy confinement time is approximately 2 times higher than the one obtained with plasma heating by the hydrogen beam and falls within the

Parameters of plasma discharges with injection of hydrogen and deuterium beams at an average density of  $5 \cdot 10^{19} \text{ m}^{-3}$

Parameter	Discharge No. 42119 (H→D)	Discharge No. 42777 (D→D)
$W_e$ , kJ	4.4	4.6
$W_i$ , kJ	4.1	7.1
$W_{th}$ , kJ	8.5	11.7
$P_{abs}^{NBI}$ , kW	850–1150	540–810
$P_i^{NBI}$ , kW	435–640	390–590
$P_e^{NBI}$ , kW	380–510	150–220
$\tau_E$ , ms	8.4–6.3	16.5–12
$\tau_E^i$ , ms	15–8.5	80–24
$\tau_E^e$ , ms	6–5	7.6–6.8
$\chi_e$ , $\text{m}^2/\text{s}$	1.2–1	1.3–1
$\chi_i$ , $\text{m}^2/\text{s}$	2.7–3.7	0.3–0.95
$\chi_i^{neo}$ , $\text{m}^2/\text{s}$	$\sim 1$	$\sim 1$
$P_{ie}$ , kW	160	300
$Z_{eff}$	3.5	3
$P_{oh}$ , kW	200	170

Note.  $W_e$ ,  $W_i$ , and  $W_{th}$  — thermal energy of electrons, ions, and their sum, respectively;  $P_{abs}^{NBI}$  — power of plasma heating by an atomic beam;  $P_e^{NBI}$  and  $P_i^{NBI}$  — power of heating of electrons and ions by an atomic beam, respectively;  $\tau_E$ ,  $\tau_E^e$ , and  $\tau_E^i$  — confinement times of the thermal energy of plasma, the electron component, and the ion component, respectively;  $\chi_e$ ,  $\chi_i$ , and  $\chi_i^{neo}$  — electron and ion thermal diffusivities and estimate of the ion neoclassical thermal diffusivity for deuterium;  $P_{ie}$  — power of electron heating in interaction with thermal ions;  $Z_{eff}$  — effective charge determined based on the measured bremsstrahlung intensity and the electron temperature and density profiles; and  $P_{oh}$  — ohmic heating power.

range of 12–16.5 ms, exceeding the IPB98(y,2) scaling by a factor of 2.

Let us consider the energy balance in the electron and ion channels. The distribution of additional heating power between electrons and ions depends on the critical energy,  $E_{crit} = 14.8 \frac{A_b}{A_{pl}^{2/3}} T_e$ . Here,  $A_b$  is the injected atom mass and  $A_{pl}$  is the ion plasma mass. When the energy of fast particles is lower than  $E_{crit}$ , plasma ions and electrons heat up at the same rate. If the energy of fast particles is higher than  $E_{crit}$ , ion heating is dominant. Since  $A_{pl}$  and  $T_e$  are equal in the considered cases,  $E_{crit}$  depends on  $A_b$  only and, consequently, differs by a factor of 2. Therefore, the distributions of absorbed beam heating power between the electron and ion components will also differ. The spatial distribution of  $T_e$  and the six-component energy composition of injected beams are taken into account in calculations performed by the NUBEAM code, which demonstrate that the power of ion heating by the beam remains largely unchanged (435–640 kW in the case of hydrogen injection and 390–590 kW for deuterium injection). This is attributable to the fact that the injected power of the hydrogen beam in the discharges chosen for comparison is higher than that of the deuterium beam. Despite this, the temperature (and, as a consequence, the energy reserve) of ions achieved in the experiment differ by a factor of almost 2. Since the ion temperature exceeds the electron one, a significant fraction of ion energy is

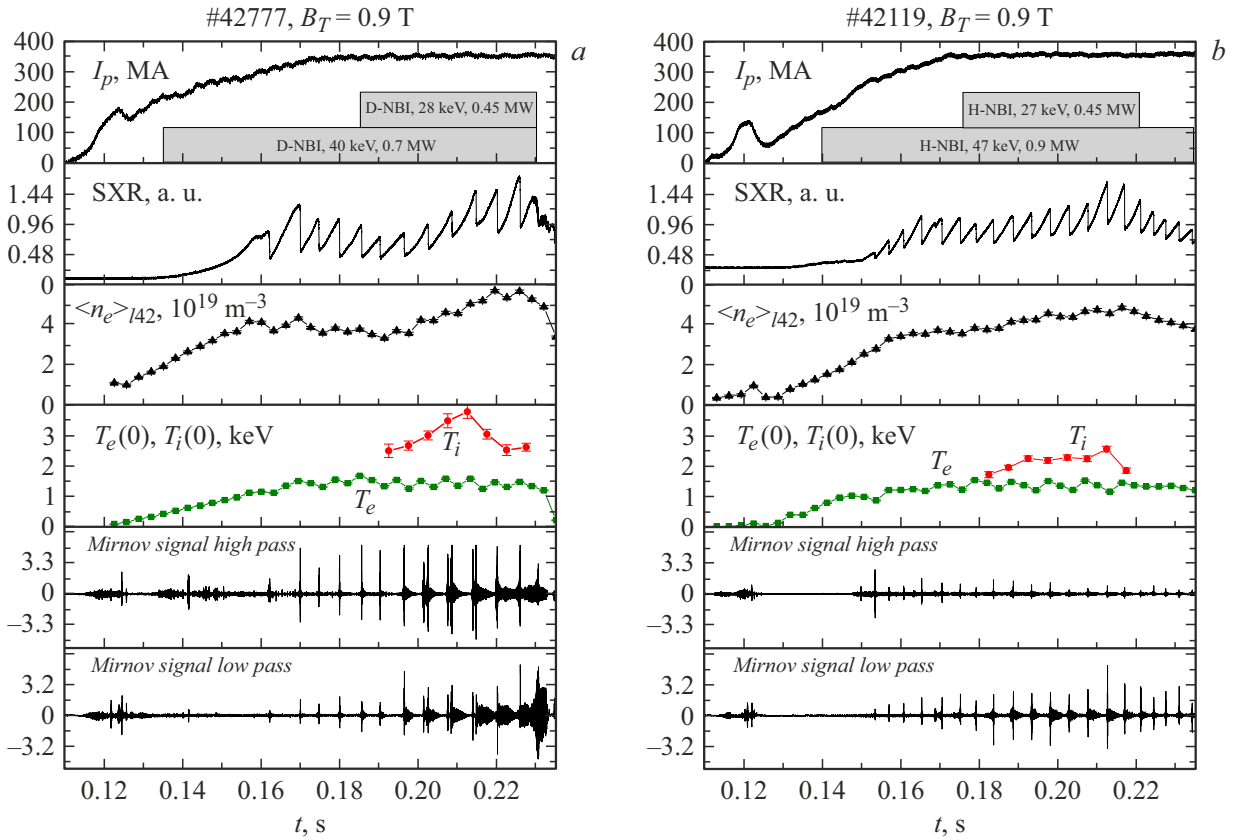


**Figure 2.** Dynamics of the main plasma parameters in discharges at the Globus-M2 tokamak with deuterium (a) and hydrogen (b) injection. From top to bottom: plasma current, soft X-ray radiation intensity, average electron density, electron and ion temperature at the center of plasma, and high-frequency and low-frequency magnetic probe signals.

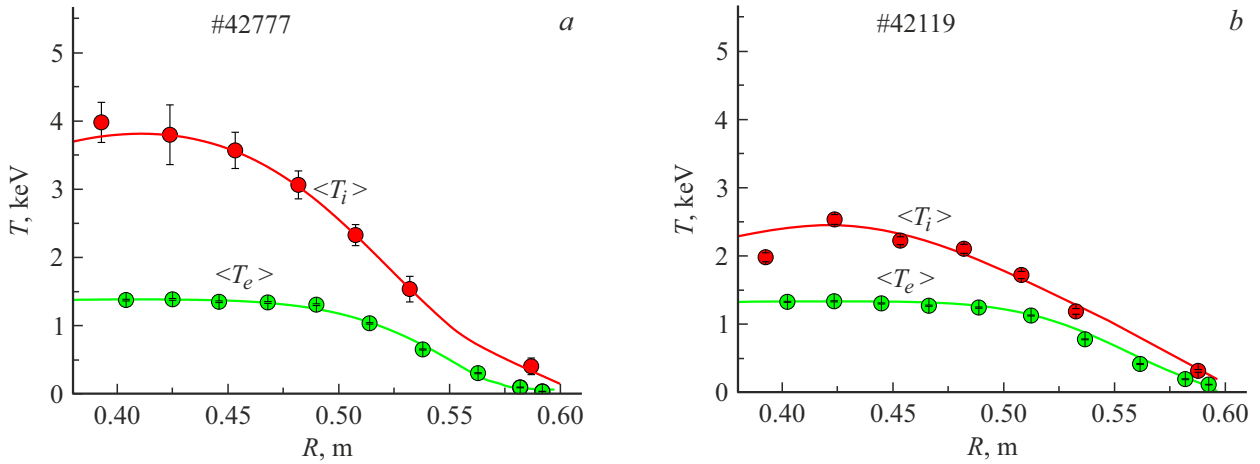


**Figure 3.** Spatial distributions of ion and electron temperatures for the Globus-M2 tokamak plasma in the deuterium (a) and hydrogen (b) injection modes averaged over 10 ms for discharge No. 42777 and over 25 ms for discharge No. 42119.

transferred to electrons as a result of Coulomb collisions. In the discharge with deuterium injection (42777), the power of heat exchange between electrons and ions is as high as 300 kW. The resulting ion heating power is just 90–290 kW and corresponds to ion energy confinement times of 24–80 ms, which are 3–5 times higher than those

corresponding to the discharge with hydrogen injection (42119). The energy stored by the electron component is the same in both cases, and the electron energy confinement times differ only slightly (approximately by 30%). A rough estimate of the electron thermal diffusivity may be obtained in the following way:  $\chi_e = a^2 \kappa (P_e - P_{rad}) / (4W_e)$ , where  $a$

and  $\kappa$  are the minor radius and elongation of the plasma column, respectively, and  $P_e$  is the total power of electron heating by the beam, thermal ions, and ohmic heating. Assuming that radiation losses  $P_{rad}$  may account for up to a half of the plasma heating power at low and moderate densities  $((2-6) \cdot 10^{19} \text{ m}^{-3})$  [11], we obtain close values of the electron thermal diffusivity. The values of ion thermal diffusivity obtained in a similar manner and the estimates derived with the use of neoclassical formulae [12] are listed in the table.

At the Globus-M2 tokamak, the injection of a deuterium beam into deuterium plasma allows one to reach significantly higher ion temperature values than those obtained when deuterium plasma is heated with a hydrogen beam. An analysis of the plasma energy balance revealed that the thermal energy confinement times differ by a factor of 2; with deuterium injection, this time is longer, reaching 12–16.5 ms at the Globus-M2 tokamak. Hydrogen beam injection is significantly less efficient due to high heat losses via the ion channel. In this case, average ion thermal diffusivity  $\chi_i$  is more than 3 times higher than the one obtained with deuterium injection, and it is also 3–4 times higher than the ion thermal diffusivity calculated in accordance with neoclassical theory (see the table). The underlying causes of the observed phenomenon are of considerable interest and warrant a more comprehensive in-depth analysis.

## Acknowledgments

Experiments were carried out at the unique scientific complex „Spherical Tokamak Globus-M,“ which is a part of the federal common research center „Material Science and Diagnostics in Advanced Technologies.“

## Funding

The calculation of the power of plasma heating by neutral injection and the analysis of the plasma energy balance were performed by the authors (G.S. Kurskiev, I.V. Miroshnikov, N.V. Sakharov, V.B. Minaev, A.Yu. Tel'nova, N.N. Bakharev, E.O. Kiselev, N.S. Zhil'tsov, P.B. Shchegolev, and E.E. Tkachenko) with financial support from the Russian Science Foundation (grant No. 24-12-00162).

## Conflict of interest

The authors declare that they have no conflict of interest.

## References

- [1] S.M. Kaye, J.W. Connor, C.M. Roach, *Plasma Phys. Control. Fusion*, **63**, 123001 (2021). DOI: 10.1088/1361-6587/ac2b38
- [2] A.A. Galeev, R.Z. Sagdeev, *Adv. Plasma Phys.*, **6**, 311 (1976). <https://ui.adsabs.harvard.edu/abs/1976app..book..311G/abstract>
- [3] M. Valovic, R. Akers, M. de Bock, J. McCone, L. Garzotti, C. Michael, G. Naylor, A. Patel, C.M. Roach, R. Scannell, M. Turnyanskiy, M. Wisse, W. Guttenfelder, J. Candy and the MAST Team, *Nucl. Fusion*, **51**, 073045 (2011). DOI: 10.1088/0029-5515/51/7/073045
- [4] S.M. Kaye, S. Gerhardt, W. Guttenfelder, R. Maingi, R.E. Bell, A. Diallo, B.P. LeBlanc, M. Podesta, *Nucl. Fusion*, **53**, 063005 (2013). DOI: 10.1088/0029-5515/53/6/063005
- [5] G.S. Kurskiev, V.K. Gusev, N.V. Sakharov, Y. Petrov, N.N. Bakharev, I.M. Balachenkov, A.N. Bazhenov, F.V. Chernyshev, N.A. Khromov, E.O. Kiselev, S.V. Krikunov, V.B. Minaev, I.V. Miroshnikov, A.N. Novokhatskii, N.S. Zhiltsov, E.E. Mukhin, M.I. Patrov, K.D. Shulyatiev, P.B. Shchegolev, O.M. Skrekel, A.Yu. Telnova, E.E. Tkachenko, E.A. Tukhmenova, V.A. Tokarev, S.Yu. Tolstyakov, V.I. Varfolomeev, A.V. Voronin, V.Yu. Goryainov, V.V. Bulanin, A.V. Petrov, A.M. Ponomarenko, A.Yu. Yashin, A.A. Kavin, E.G. Zhilin, V.A. Solovey, *Nucl. Fusion*, **62**, 016011 (2022). DOI: 10.1088/1741-4326/ac38c9
- [6] G.S. Kurskiev, N.V. Sakharov, V.K. Gusev, V.B. Minaev, I.V. Miroshnikov, Y. Petrov, A. Telnova, N.N. Bakharev, E.O. Kiselev, N.S. Zhiltsov, P.B. Shchegolev, I.M. Balachenkov, V.I. Varfolomeev, A.V. Voronin, V.Yu. Goryainov, V.V. Dyachenko, E.G. Zhilin, M.V. Iliasova, A.A. Kavin, A.N. Konovalov, S.V. Krikunov, K.M. Lobanov, A.D. Melnik, A.B. Mineev, A.N. Novokhatsky, M.I. Patrov, A.V. Petrov, A.M. Ponomarenko, O.M. Skrekel', V.A. Solovei, V.V. Solokha, E.E. Tkachenko, V.A. Tokarev, S.Yu. Tolstyakov, E.A. Tukhmenova, E.M. Khilkevitch, N.A. Khromov, F.V. Chernyshev, A.E. Shevelev, K.D. Shulyatev, A.Yu. Yashin, *Plasma Phys. Rep.*, **49**, 403 (2023). DOI: 10.1134/S1063780X23600214
- [7] G.S. Kurskiev, I.V. Miroshnikov, N.V. Sakharov, V.K. Gusev, Y. Petrov, V.B. Minaev, I.M. Balachenkov, N.N. Bakharev, F.V. Chernyshev, V.Yu. Goryainov, A.A. Kavin, N.A. Khromov, E.O. Kiselev, S.V. Krikunov, K.M. Lobanov, A.D. Melnik, A.N. Novokhatskii, S.V. Filippov, N.S. Zhiltsov, A.B. Mineev, E.E. Mukhin, M.I. Patrov, A.V. Petrov, A.M. Ponomarenko, V.V. Solokha, K.D. Shulyatiev, P.B. Shchegolev, O.M. Skrekel, A.Yu. Telnova, E.E. Tkachenko, E.A. Tukhmenova, V.A. Tokarev, S.Yu. Tolstyakov, V.I. Varfolomeev, A.V. Voronin, A.Yu. Yashin, V.A. Solovey, E.G. Zhilin, *Nucl. Fusion*, **62**, 104002 (2022). DOI: 10.1088/1741-4326/ac881d
- [8] S.A.M. McNamara, O. Asunta, J. Bland, P.F. Buxton, C. Colgan, A. Dnestrovskii, M. Gemmell, M. Gryaznevich, D. Hoffman, F. Janky, J.B. Lister, H.F. Lowe, R.S. Mirfayzi, G. Naylor, V. Nemytov, J. Njau, T. Pyragius, A. Rengle, M. Romanelli, C. Romero, M. Sertoli, V. Shevchenko, J. Sinha, A. Sladkomedova, S. Sridhar, Y. Takase, P. Thomas, J. Varje, B. Vincent, H.V. Willett, J. Wood, D. Zakhar, D.J. Battaglia, S.M. Kaye, L.F. Delgado-Aparicio, R. Maingi, D. Mueller, M. Podesta, E. Delabie, B. Lomanowski, O. Marchuk and the ST40 Team, *Nucl. Fusion*, **63**, 054002 (2023). DOI: 10.1088/1741-4326/acbec8
- [9] S.M. Kaye, M. Sertoli, P. Buxton, A. Dnestrovskii, S. McNamara, M. Romanelli, P. Thomas, *Plasma Phys. Control. Fusion*, **65**, 095012 (2023). DOI: 10.1088/1361-6587/ace849
- [10] A. Pankin, D. McCune, R. Andre, G. Bateman, A. Kritiz, *Comput. Phys. Commun.*, **159**, 157 (2004). DOI: 10.1016/j.cpc.2003.11.002

- [11] E.A. Tikhmeneva, N.N. Bakharev, V.I. Varfolomeev, V.K. Gusev, N.S. Zhiltsov, E.O. Kiselev, G.S. Kurskiev, V.B. Minaev, Yu.V. Petrov, N.V. Sakharov, A.D. Sladkomedova, A.Yu. Telnova, S.Yu. Tolstyakov, P.B. Shchegolev, *Tech. Phys. Lett.*, **47**, 56 (2021). DOI: 10.1134/S1063785021010272.
- [12] W.A. Houlberg, K.C. Shaing, S.P. Hirshman, M.C. Zarnstorff, *Phys. Plasmas*, **4**, 3230 (1997). DOI: 10.1063/1.872465

*Translated by D.Safin*